Ecological Complexity 34 (2018) 139–146

Contents lists available at ScienceDirect

Ecological Complexity

journal homepage: www.elsevier.com/locate/ecocom

Original Research Article

# Quantifying species extinction risk under temporal environmental variance

Tak Fung[a], James P. O'Dwyer[b], Ryan A. Chisholm[a,c,*]

[a] National University of Singapore, Department of Biological Sciences, 14 Science Drive 4 Singapore 117543, Singapore
[b] University of Illinois, School of Integrative Biology, Department of Plant Biology, 505 S. Goodwin Avenue, Urbana, IL 61801, USA
[c] Smithsonian Tropical Research Institute, Balboa, Ancón, Panama

ARTICLE INFO

*Article history:*
Received 15 November 2016
Revised 11 May 2017
Accepted 28 September 2017
Available online 13 October 2017

*Keywords:*
Biodiversity
Environmental variance
Extinction time
Markov chain
Species lifetime

ABSTRACT

Species populations are subjected to fluctuations in their surrounding environment, and the strength of these fluctuations has been hypothesized to be a major determinant of the extinction risk of these populations. Therefore, a key question is: How does temporal environmental variance affect the extinction risk of species populations? Previous theory based on the dynamics of single populations typically predicts an increased risk of extinction from the effects of environmental variance. However, previous studies have focused mainly on the case where environmental effects are temporally uncorrelated (white environmental noise), whereas such effects are typically correlated (colored environmental noise) in nature. Thus, further work on the case of colored environmental noise is required, but this has been hindered by the analytical intractability of corresponding stochastic models. In our study, we address this limitation by developing a new discrete-time Markov chain model of a species population fluctuating under colored environmental noise, with the simplification that the effects of demographic variance are manifested indirectly as an extinction threshold. This simplifying assumption allows us to derive analytical solutions, which show that the expected extinction time of model species declines with the strength of environmental variance under a variety of different scenarios, reflecting greater extinction risk. Our study thus clarifies the situations under which environmental variance tends to increase extinction risk, and provides a novel analytically tractable framework for modeling temporal environmental variance. We also discuss the possible implications of our results for species richness in ecological communities.


## 1. Introduction

Ecology aims to develop and test hypotheses about the processes that structure biodiversity in ecosystems across the world. A major driver of ecological dynamics is temporal environmental variance, which affects all ecological communities to some degree. Examples include the effects of forest fires (Ahlgren and Ahlgren, 1960; Turcq et al., 1998), tropical storms impacting coral reef ecosystems (Connell, 1997; Gardner et al., 2005) and human harvesting (Jackson et al., 2001; Ceballos et al., 2015). Temporal environmental variance is likely to increase in the future, especially given future projections of increased variance under continued climate change (Knapp et al., 2008), and this provides an additional motive for understanding its effects on ecological communities and the populations of species that comprise them. Furthermore, temporal environmental variance has been found to be important for correcting the gross underestimates of temporal changes in biodiversity by neutral models (Nee, 2005; Chisholm and O'Dwyer, 2014; Chisholm et al., 2014; Kalyuzhny et al., 2015; Fung et al., 2016a).

Early population models showed how temporal environmental variance (hereafter, "environmental variance") can increase the extinction risk of species populations (Leigh, 1981; Lande, 1993; Foley, 1994). These predictions have partial support from empirical data. For example, time-series analyses of 53 temperate lakes in North America and Europe found that larger fluctuations in pH, phosphorus and dissolved organic carbon were associated with fewer species of zooplankton (Shurin et al., 2010). Similar processes may operate over geological timescales: regions with historically stable climates, such as the tropics and the Cape Floris-

* Corresponding author.
*E-mail addresses:* tfung2000@gmail.com (T. Fung), jodwyer@illinois.edu (J.P. O'Dwyer), ryan.chis@gmail.com (R.A. Chisholm).

https://doi.org/10.1016/j.ecocom.2017.09.006
1476-945X/

tic Region of South Africa, tend to have higher present-day floristic diversity and this has been attributed to lower extinction rates (Wallace, 1878; Huntley et al., 2014).

A limitation of the early theoretical results on this topic (Leigh, 1981; Lande, 1993; Foley, 1994) is that they were derived from models that assumed environmental effects are uncorrelated or largely uncorrelated in time, which correspond to the case of white environmental noise. However, environmental variables have often been found to exhibit substantial positive correlations over timescales of days to millennia (Steele, 1985; Inchausti and Halley, 2002), which correspond to colored environmental noise (Halley, 1996). Examination of the case of colored environmental noise has been hampered by a lack of analytical tractability in corresponding stochastic models (Ovaskainen and Meerson, 2010). For colored environmental noise, Kamenev et al., 2008 derived an analytical formula for expected extinction time, but only when the temporal correlation in environmental effects are very large. In contrast, Fung et al. (2016b) analyzed a master-equation model that incorporated colored environmental noise with any degree of temporal correlation, and derived formulae specifying the expected species lifetime. Using these formulae, they found that expected species lifetime increased with the degree of temporal correlation for specific sets of species demographic rates, implying lower extinction risk when environmental noise was colored instead of white (Fung et al., 2016b). But the formulae were complicated and did not provide a clear, general understanding of how extinction risk changed with different regimes of environmental variance.

Given the variety of predictions from models with environmental variance, a current research priority is to establish quantitative criteria for predicting the conditions under which environmental variance increases or decreases extinction risk, particularly in the case of colored environmental noise. To address this need, we develop here a new analytically tractable model describing the nonlinear dynamics of a population exposed to fluctuating environmental disturbances, which may exhibit weak to strong correlations in time. Afterwards, we analyze the model to show how extinction risk in the model typically increases with the strength of environmental variance, conceptualized as the degree to which environmental factors change the population growth rates of species over time. We conclude by relating our results to those of previous models and discussing general implications for the role of environmental variance in shaping the persistence of species populations and hence biodiversity.

## 2. Methods

### 2.1. Model description: biological perspective

We begin by constructing a population model that describes how the abundance of a species fluctuates under random changes in the environment. We choose to represent the dynamics using a discrete-time Markov chain process because this allows temporally correlated environmental effects on species abundance to be represented simply as transition probabilities, integrating the correlated effects over a discrete time-step. At the end of each time-step, the environmental regime randomly changes, such that environmental effects are uncorrelated between time-steps. In addition, representation of our model using a discrete-time Markov chain allows us to take advantage of mathematical theory available for computing the expected extinction time of a model species (Brémaud, 1999). The model represents the abundance of a species on a log-scale to allow simpler representation of the transition probabilities. Technically, the log-abundance of a species extends to negative infinity and never reaches a value corresponding to an abundance of zero; therefore, it is necessary to impose a log-abundance extinction threshold below which the effects of demographic variance are implicitly assumed to cause extinction. Following classic population models with environmental variance (Leigh, 1981; Lande, 1993; Foley, 1994), we set a log-abundance of zero as the extinction threshold, which corresponds to an abundance of one on a linear scale. Furthermore, again following classic population models (Leigh, 1981; Lande, 1993; Foley, 1994), a carrying capacity is imposed on each species population. This implicitly represents negative density-dependence caused by processes such as resource limitation, intraspecific competition and density-dependent predation (e.g., Janzen, 1970; Connell, 1971; Harms et al., 2000; Webb et al., 2006; Comita et al., 2010; Bagchi et al., 2014).

In the first version of our model, the log-abundance of the model species is assumed to fluctuate according to a truncated symmetric Laplace distribution (SLD) (also referred to as a symmetric double-exponential distribution), where the truncation is from above, with the maximum value representing the species carrying capacity. In the second version of the model, the log-abundance is assumed to fluctuate according to a truncated asymmetric Laplace distribution (ALD), which allows greater flexibility over how environmental variance affects species abundance. The ALD includes the SLD as a specific instance, when the asymmetry is zero. Our choice of an ALD is based on the reasonably good fits that it provides to changes in tree species abundances in 12 temperate and tropical forest communities around the world (Chisholm et al., 2014).

Fig. 1 shows a schematic diagram of our model, highlighting the key biological processes modeled.

### 2.2. Model description: mathematical perspective

In the first version of the model, during one time-step, the probability of the model species transitioning from log-abundance $y$ given that it has log-abundance $x$ is defined by the probability distribution function (pdf)

$$f_1(y|x) = B_1 \exp(-\gamma|x-y|), \tag{1}$$

where the parameter $\gamma$ measures the rate of decay of the probability density either side of $x$ and $-\infty < x,\ y \leq A$. Here, $A$ is the maximum abundance on a log-scale with base $a$, so that $K = a^A$ is the maximum abundance on a linear scale, i.e. the species' carrying capacity. Also, the parameter $B_1$ is a normalization constant given by

$$B_1 = \frac{\gamma}{2 - e^{\gamma(x-A)}}. \tag{2}$$

Eq. (1) is the pdf of a truncated SLD (Fig. 2). It can be shown that the smaller the value of $\gamma$, i.e. the greater the value of $1/\gamma$, the greater the expected absolute change in log-abundance over one time-step (Appendix A in Supplementary material). Furthermore, it can be shown that the greater the value of $1/\gamma$, the greater the expected deviation of the instantaneous population growth rate from zero in one time-step (Appendix A in Supplementary material) – this growth rate reflects the net balance of the rate at which new individuals are recruited and the rate at which existing individuals die, and changes randomly across time-steps (Appendix A in Supplementary material). Together, these results imply that $1/\gamma$ is a measure of the strength of environmental variance on changes in species abundance, as mediated by changes in key demographic rates.

To permit application of Markov chain theory for discrete-time processes with discrete states, we sample the continuous log-abundance scale at equidistant points (later, after derivation of formulae for extinction times, we move back onto the continuous log-abundance scale by taking the limit as the distance between points approaches zero). Specifically, let there be an infinite number of discrete states (log-abundances) spread equally from $A$

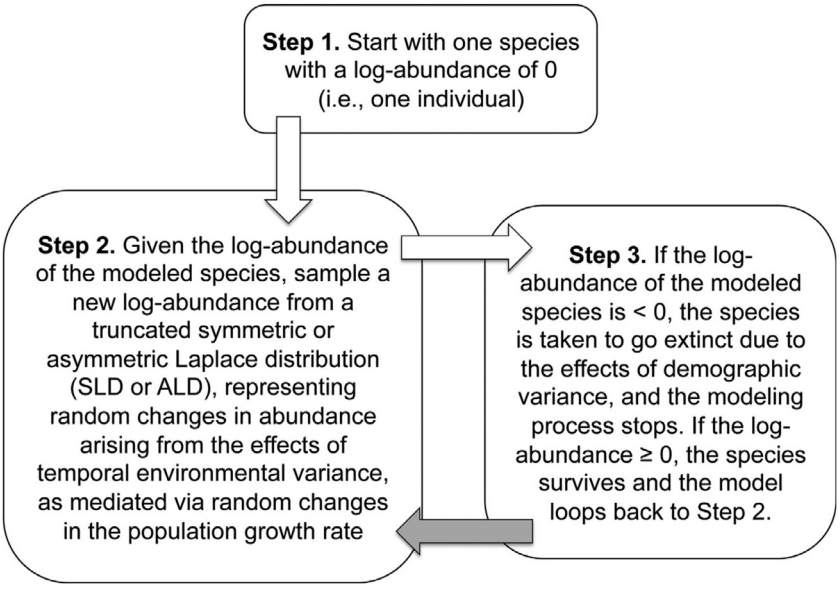


**Fig. 1.** Schematic diagram of our model, showing the key steps and biological processes. The model starts with one species that has one individual and applies successive changes in species' abundance arising from the effects of temporal environmental variance, until the species goes extinct. The gray arrow represents a transition that occurs only if the condition in Step 3 (the species has at least one individual) is satisfied. The use of a truncated SLD or ALD corresponds to the two versions of the model.

downwards, with state $i \in \{\ldots, -1, 0, 1, \ \ldots, \ k\}$ corresponding to log-abundance $iA/k$. States $i < 0$ correspond to absorbing states because they correspond to abundances below one on a linear scale, which is the threshold below which extinction is taken to occur. On the discrete log-abundance scale, the probability of a species transitioning from non-absorbing state $i$ to a state $j$ (which can be non-absorbing or absorbing) is defined by the probability mass function (pmf)

$$\zeta_1(j|i) = \frac{f_1(jA/k|iA/k)\delta y}{\sum_{m=-\infty}^{k} f_1(mA/k|iA/k)\delta y} = \frac{e^{-\lambda|i-j|}\left(1-e^{\lambda}\right)}{e^{\lambda(i-k)}-1-e^{\lambda}}, \tag{3}$$

where $\lambda = \gamma A/k$.

The second version of the model is the same as the first except that the pdf specifying transition probabilities is a truncated ALD rather than a truncated SLD:

$$f_2(y|x) = \begin{cases} B_2\exp(-\gamma_1|x-y|) & \text{for} \quad -\infty \le y < x \\ B_2\exp(-\gamma_2|x-y|) & \text{for} \quad x \le y \le A \end{cases}, \tag{4}$$

where $B_2$ is a normalization constant given by

$$B_2 = \frac{\gamma_1\gamma_2}{\gamma_1+\gamma_2-\gamma_1 e^{\gamma_2(x-A)}} \tag{5}$$

(Fig. 3). It can be shown that the larger $1/\gamma_1$ or $\gamma_2$ is, the smaller the expected log-abundance at the end of a time-step, given a log-abundance at the beginning of the time-step (Appendix A in Supplementary material). To simplify our analyses, we henceforth assume that environmental variance acts on $\gamma_1$ and $\gamma_2$ simultaneously, changing both in the same direction and by proportionally the same amount. This means that the ratio $\gamma_2/\gamma_1 = \alpha$ is preserved, allowing us to write $\gamma_1 = \gamma$ and $\gamma_2 = \alpha\gamma$. The case $\alpha = 1$ corresponds to the first version of the model, so in the ALD context we examine only cases where $\alpha \neq 1$. Given the interpretation of $\gamma_1$ and $\gamma_2$ above, we see that $\alpha = (1/\gamma_1)\gamma_2$ measures the

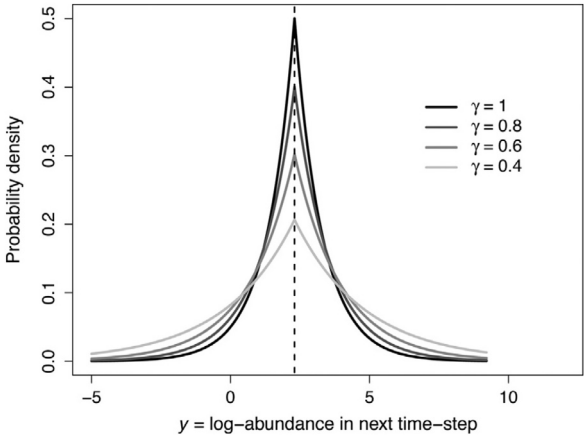


**Fig. 2.** Symmetric Laplace distributions specified by (1) and (2), with $a = e$, $x = \log_e(10) = 2.30$, $A = \log_e(10{,}000) = 9.21$ and $\gamma = 1$, 0.8, 0.6 and 0.4. The distributions are truncated from above at $y = A$. In addition, the vertical dashed line marks the log-abundance in the current time-step ($x$).

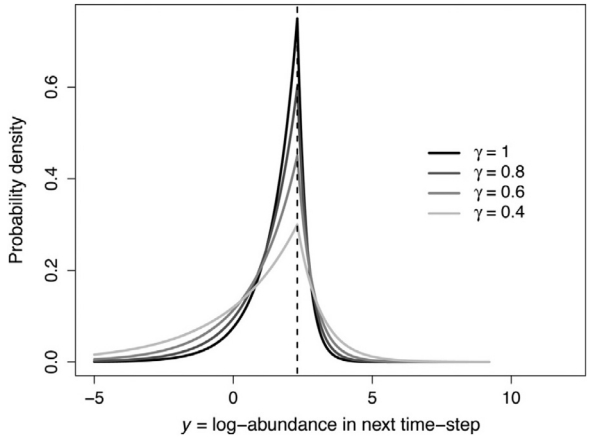


**Fig. 3.** Asymmetric Laplace distributions specified by (4) and (5), with $a = e$, $x = \log_e(10) = 2.30$, $A = \log_e(10{,}000) = 9.21$, $\alpha = \gamma_2/\gamma_1 = 3$ and $\gamma = \gamma_1 = 1$, 0.8, 0.6 and 0.4. The distributions are truncated from above at $y = A$. In addition, the vertical dashed line marks the log-abundance in the current time-step ($x$).

tendency of the species log-abundance to decrease, given an initial value. With this re-parameterization, it can be shown that both the expected absolute change in log-abundance over one time-step and the expected deviation of the instantaneous population growth rate from zero in one time-step decrease with $\gamma$, for all $\alpha > 0.0458$ (Appendix A in Supplementary material). Therefore, as in the first version of the model, for this range of $\alpha$, $1/\gamma$ can be used as a measure of the strength of environmental variance, as mediated by changes in key demographic rates and reflected in changes in species abundance. For small values of $\alpha \leq 0.0458$ that represent extreme ALD distributions with relatively high probability density for log-abundances higher than the current value, the expected absolute change in log-abundance and deviation of the instantaneous population growth rate are not guaranteed to decrease with $\gamma$ for all values of $\gamma$, such that $1/\gamma$ cannot be unambiguously interpreted as the strength of environmental variance. Therefore, we only consider the range $\alpha > 0.0458$ in our analyses of the model. In this case, as $1/\gamma$ increases, the log-abundance at the end of a time-step tends to deviate more from its value at the beginning of the time-step (Fig. 3). We note that as $1/\gamma$ increases, the probability of achieving more extreme log-abundances either side of the current log-abundance increases (Fig. 3), such that it is unclear what the net effect on extinction times are without performing explicit calculations.

As in the first version of the model, the pdf can be discretized to give the following pmf:

$$\zeta_2(j|i) = \begin{cases} \dfrac{e^{-\lambda|i-j|}\left(1 - e^{\lambda} - e^{\alpha\lambda} + e^{(1+\alpha)\lambda}\right)}{e^{-\alpha(k-i)\lambda} - e^{\lambda-\alpha(k-i)\lambda} + e^{(1+\alpha)\lambda} - 1} & \text{for} \quad j \leq i \\ \dfrac{e^{-\alpha\lambda|i-j|}\left(1 - e^{\lambda} - e^{\alpha\lambda} + e^{(1+\alpha)\lambda}\right)}{e^{-\alpha(k-i)\lambda} - e^{\lambda-\alpha(k-i)\lambda} + e^{(1+\alpha)\lambda} - 1} & \text{for} \quad j > i \end{cases}. \tag{6}$$

### 2.3. Deriving analytical expressions for expected extinction time as functions of environmental variance

We first derive a formula for the expected lifetime of a species in our model. The expected species lifetime measures the expected length of time between the appearance of a new singleton species in the model and the eventual extinction of this species. Thus, it is the same as the expected time to extinction of a species with an initial abundance of one, and we denote it by $T_1$. To derive a formula for $T_1$ from our model, first define $\mathbf{P}$ to be the transition probability matrix, with $ij$th entry $p_{ij} = \zeta_1(j|i)$ or $\zeta_2(j|i)$. Let $\mathbf{Q}$ be the matrix obtained by deleting the rows and columns of $\mathbf{P}$ corresponding to the absorbing states, such that $\mathbf{Q}$ is the probability matrix of transitions between transient states. Then the fundamental matrix is defined to be

$$\mathbf{N} = (\mathbf{I} - \mathbf{Q})^{-1} \tag{7}$$

(Brémaud, 1999). The first row of $\mathbf{N}$ is

$$\mathbf{h} = \mathrm{e}_1\mathrm{N}, \tag{8}$$

where $\mathbf{e}_1$ is the unit row vector $(1, 0, 0, \ldots, 0)$. The significance of $\mathbf{h}$ is that its $(i+1)$th entry is the expected number of times transient state $i$ will be hit before absorption (extinction), assuming we start in state 0 (i.e., an abundance of $a^0 = 1$). Thus,

$$T_1 = \sum_{i=1}^{k} h_i, \tag{9}$$

where $T_1$ is measured as the expected number of time-steps during the lifetime of a model species. To derive analytical expressions for the entries in $\mathbf{h}$, we explicitly calculate the entries in $\mathbf{h}$ for small values of $k$, formulate candidate expressions for general $k$, and then prove that they satisfy (7) and (8). We substitute these expressions into (9) and then take the continuous abundance limit to move back to the continuous abundance scale for which the model was first formulated. We then examine the resulting expression to determine how species lifetime is predicted to vary with changing strength of environmental variance under the two versions of the model.

Secondly, we derive a formula for the expected (or mean) time to extinction of a species in our model, when it starts with an abundance equal to the species carrying capacity $K$ (i.e. when it starts in state $k$). We denote this expected time to extinction as $T_K$. Formulae for $T_K$ have been commonly calculated for previous population models (Leigh, 1981; Lande, 1993; Foley, 1994; Kamenev et al., 2008), which all use diffusion approximations. Deriving a formula specifying $T_K$ for our model allows us to better connect our model with these previous models. To do this, we note that the last row of $\mathbf{N}$ is

$$\mathrm{g} = \mathrm{e}_k\mathrm{N}, \tag{10}$$

where $\mathbf{e}_k$ is the unit row vector $(0, 0, \ldots, 0, 1)$. Analogous to $\mathbf{h}$, the $(i+1)$th entry in $\mathbf{g}$ is the expected number of times transient state $i$ will be hit before absorption, assuming we start in state $k$. Thus,

$$T_K = \sum_{i=1}^{k} g_i. \tag{11}$$

For the first version of our model, analytical expressions for the entries in $\mathbf{g}$ are derived as for entries in $\mathbf{h}$, and substituted into (11). The resulting summation is then simplified by taking the continuous abundance limit, to derive an analytical expression for $T_K$. This method worked for the first version of our model (the SLD) but not for the second version (the ALD) because it resulted in a summation in (11) that could not be simplified in the continuous abundance limit. Therefore, we do not consider derivation of $T_K$ for the second version of our model.

## 3. Results

### 3.1. First version of model: expected species lifetime

In the first version of the model, the changes in species log-abundances are specified by a truncated SLD, as given by (1)–(3). Based on explicit calculations of entries in the first row of the fundamental matrix, $\mathbf{h}$, for small values of the number of states with abundances greater than the extinction threshold of one, $k$, we formulate the following ansatz for general $k$:

$$h_0 = e^{\lambda}, \tag{12a}$$

$$h_i = \frac{e^{i\lambda}\left(-1 + e^{\lambda} + e^{(k-i)\lambda} - e^{(k-i+2)\lambda}\right)}{1 - e^{k\lambda} - e^{(k+1)\lambda}} \quad \text{for } i = 1, 2, \ldots, k-1, \tag{12b}$$

$$h_k = \frac{e^{(k+1)\lambda}\left(1 - e^{\lambda}\right)}{1 - e^{k\lambda} - e^{(k+1)\lambda}}. \tag{12c}$$

To prove that (12a)–(12c) are correct, it is sufficient to show that they satisfy (7) and (8). In Appendix B of the Supplementary material, we show that (12a)–(12c) do indeed satisfy (7) and (8). Substituting (12a-c) into the formula for the expected species lifetime $T_1$, (9), gives:

$$T_1 = \sum_{i=0}^{k} h_i = \frac{e^{k\lambda}\left(-k + e^{2\lambda}(k+1)\right)}{-1 + e^{k\lambda} + e^{(k+1)\lambda}}. \tag{13}$$

To simplify (13), we take the continuous abundance limit – this occurs when the spacing between the discrete log-abundance classes,

$1/k$, tends to zero and is equivalent to taking the limit $k \to \infty$. In this limit, $T_1 \to T_{1,C}$, where

$$T_{1,C} = \frac{e^{\lambda'}\left(1+2\lambda'\right)}{\left(-1+2e^{\lambda'}\right)} \approx \lambda' \tag{14}$$

for sufficiently large $\lambda'$. This formula directly relates species lifetime $T_{1,C}$ to the environmental variance parameter $\lambda' = \gamma A$, and is a key result of our study. Because $\lambda'$ is directly proportional to $\gamma$, we can interpret $1/\lambda'$ as a measure of the strength of environmental variance, in the same way as $1/\gamma$.

### 3.2. First version of model: how expected species lifetime changes with environmental variance

The formula we derived for $T_{1,C}$ in the previous subsection (3.1) allows us to quantitatively examine how expected species lifetime changes with the strength of environmental variance $1/\lambda'$. We have:

$$\frac{dT_{1,C}}{d\lambda'} = \frac{e^{\lambda'}\left(-3-2\lambda'+4e^{\lambda'}\right)}{\left(1-2e^{\lambda'}\right)^2}. \tag{15}$$

The numerator is positive for $\lambda' > 0$ and hence $dT_{1,C}/d\lambda' > 0$, such that $dT_{1,C}/d(1/\lambda') < 0$ – expected species lifetime decreases with $1/\lambda'$. For sufficiently large $\lambda'$, $T_{1,C} \approx \lambda'$ (from (14)) and hence expected species lifetime decreases almost linearly with $1/\lambda'$ on double-log axes. Fig. 4 shows that the linearly decreasing trend for $T_{1,C}$ holds over a wide range of $1/\lambda'$ from $10^{-8}$ to approximately 1, whereupon $T_{1,C}$ flattens out at 1, as predicted by (14).

### 3.3. First version of model: expected time to extinction starting at the species carrying capacity

Analogous to our derivation of entries in **h**, we formulate and prove the following ansatz for entries in the last row of the fundamental matrix, **g**:

$$g_0 = -1 + e^{\lambda}, \tag{16a}$$

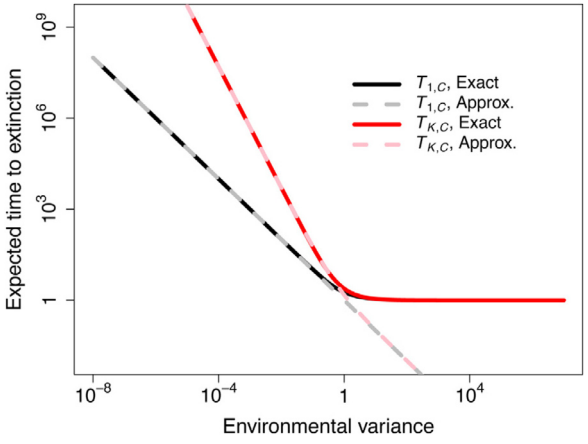


**Fig. 4.** Changes in expected extinction time for a species with initial abundance equal to one ($T_{1,C}$, also called the expected species lifetime) or the maximum value $K$ ($T_{K,C}$), with increasing strength of environmental variance ($1/\lambda'$). The changes in species log-abundances are specified by a truncated SLD. For this graph, the exact and approximate values of $T_{1,C}$ are computed using (14), with the approximate values defined by $T_{1,C} \approx \lambda'$. Also, the exact and approximate values of $T_{K,C}$ are computed using (17), with the exact values calculated numerically using the summation in (17) (Appendix C in Supplementary material) and the approximate values of $T_{K,C}$ defined by $T_{K,C} \approx \lambda' + [(\lambda')^2/2]$.

$$g_i = -2(i+1) + 1 + (i+1)e^{\lambda} + \sum_{j=1}^{i} \frac{-2 + e^{\lambda} - e^{(j-1)\lambda} + 2e^{j\lambda} - e^{(j+1)\lambda} + e^{(k-i+j-1)\lambda} + e^{(k-i+j)\lambda}}{-1 + e^{(k-i+j)\lambda} + e^{(k-i+j+1)\lambda}}$$
$$\text{for } i = 1, \ldots, k-1, \tag{16b}$$

$$g_k = -3k + (k+1)e^{\lambda} + \sum_{j=1}^{k} \frac{-3 + e^{\lambda} + 4e^{j\lambda}}{-1 + e^{j\lambda} + e^{(j+1)\lambda}} \tag{16c}$$

(Appendix C in Supplementary material). Using (16a)–(16c) and taking the continuous abundance limit, we can show that for sufficiently large $\lambda'$, the expected time to extinction starting at the species carrying capacity (or maximum species abundance) $K$ is

$$T_K = \sum_{i=0}^{k} g_i \to T_{K,C} \approx \lambda' + \frac{(\lambda')^2}{2} \tag{17}$$

(Appendix C in Supplementary material). Also, for $\lambda' = 0$, $\lambda = \lambda'/k = 0$. Hence, from (16a)–(16c), $g_0 = g_i = 0$ and $g_k = 1$, such that $T_K = T_{K,C} = 1$. This means that as $\lambda' \to 0$, $T_{K,C} \to 1$. Fig. 4 shows that $T_{K,C}$ closely follows the approximation (17) over a wide range of $1/\lambda'$ up to approximately 1, whereupon $T_{K,C}$ flattens out at 1, as predicted. When $\lambda'$ is large enough such that the second term in the approximation in (17) dominates, $T_{K,C}$ scales with $(\lambda')^2 = (\log K)^2/(1/\gamma)^2$, in contrast to the scaling with $\lambda'$ found for $T_{1,C}$. To help interpret this scaling relationship biologically, it can also be shown that for sufficiently large $\lambda'$, the parameter $1/\gamma$ is a good approximation of the expected absolute change in log-abundance over one time-step, considering the lifetime of one species (Appendix C in Supplementary material). In this case, $(1/\gamma)^2$ can be interpreted as the square of this expected change, which measures how much the square of the log-abundance deviates in one time-step from its initial value and is therefore similar to the variance of log-abundance due to environmental effects.

### 3.4. Second version of model with asymmetric transition probability matrix

In the second version of the model, the changes in species log-abundances are specified by a truncated ALD. Using the same method that we applied to the first version of the model, we can prove that the entries in the first row of the fundamental matrix for the second version of the model are specified by

$$h_0 = e^{\lambda_1}, \tag{18a}$$

$$h_i = \frac{e^{i\lambda}\left(-1+e^{\lambda}\right)\left(1-e^{\lambda}-e^{(k-i)\alpha\lambda}+e^{\lambda+(k-i+1)\alpha\lambda}\right)}{1-e^{\lambda}-e^{k\alpha\lambda}+e^{\lambda+(k+1)\alpha\lambda}},$$
$$\text{for } i = 1, 2, \ldots, k-1, \tag{18b}$$

$$h_{k-1} = \frac{e^{(k-1)\lambda}\left(1-e^{\lambda}\right)\left(1-e^{\alpha\lambda}\right)\left(-1+e^{\lambda}+e^{(1+\alpha)\lambda}\right)}{1-e^{\lambda}-e^{k\alpha\lambda}+e^{\lambda+(k+1)\alpha\lambda}}, \tag{18c}$$

$$h_k = \frac{e^{(k+1)\lambda}\left(-1+e^{\lambda}\right)\left(-1+e^{\alpha\lambda}\right)}{1-e^{\lambda}-e^{k\alpha\lambda}+e^{\lambda+(k+1)\alpha\lambda}} \tag{18d}$$

(Appendix B in Supplementary material). Here, $\alpha$ measures the degree of asymmetry in the ALD. Substituting (18a)–(18d) into the

formula for $T_1$ (9) and then taking the continuous abundance limit gives

$$T_{1,C} = \frac{\alpha\left(2e^{\lambda'} - (1+\alpha)e^{\alpha\lambda'}\right)}{(1-\alpha)\left((1+\alpha)e^{\alpha\lambda'} - 1\right)}, \tag{19}$$

From (19),

$$\frac{dT_{1,C}}{d\lambda'} = \frac{\alpha\left[2e^{\lambda'} + e^{\alpha\lambda'}\left(2e^{\lambda'}(-1+\alpha) - \alpha\right)(1+\alpha)\right]}{(-1+\alpha)\left((1+\alpha)e^{\alpha\lambda'} - 1\right)}. \tag{20}$$

It can be shown that for all $\alpha < 1$ and $\alpha > 1$, $dT_{1,C}/d(1/\lambda') < 0$ and hence species lifetime decreases with $1/\lambda'$ as in the first version of the model (Appendix D in Supplementary material; Fig. 5). In addition, $T_{1,C}$ is greater than $T_{1,C}$ from the first model (SLD; $\alpha = 1$) when $\alpha < 1$ and less when $\alpha > 1$ (Appendix E in Supplementary material; Fig. 5). This means that if environmental variance tends to increase the log-abundance of a species by a greater amount than in the first version of the model ($\alpha < 1$), then expected species lifetime increases, and vice versa. Furthermore, because of the factor $e^{\alpha\lambda'}$ in the expression for $T_{1,C}$, for sufficiently large $\lambda'$ (i.e. sufficiently small $1/\lambda'$), $T_{1,C}$ changes rapidly as $\alpha$ deviates from 1 (see Fig. 5, with $\alpha = 0.999$ and 1.0001).

### 3.5. Implications of results for species richness in the null case with no interspecific interactions

The extinction time results that we derived using our population model can be used to inform how species richness changes with environmental variance in idealized communities with no interspecific interactions. Although such idealized communities are not found in reality, they may nonetheless serve as useful null models that can be compared with more complex models to elucidate processes driving patterns of biodiversity. A key example of such a null community model is the non–zero-sum neutral model (with no temporal environmental variance), which consists of species populations with the same demographic rates and fluctuating independently under neutral drift. This model has been analyzed to provide null expectations of key patterns of biodiversity such as species-abundance distributions and extinction times (Volkov et al., 2003; Volkov et al., 2007; Chisholm and ODwyer, 2014). We also note that for large community sizes, the non-zero-sum neutral model can be used to approximate a zero-sum model with species indirectly competing for a fixed amount of resources (Chisholm and O'Dwyer, 2014). This shows how a model with non-interacting species might be used to approximate a model with interacting species under particular circumstances.

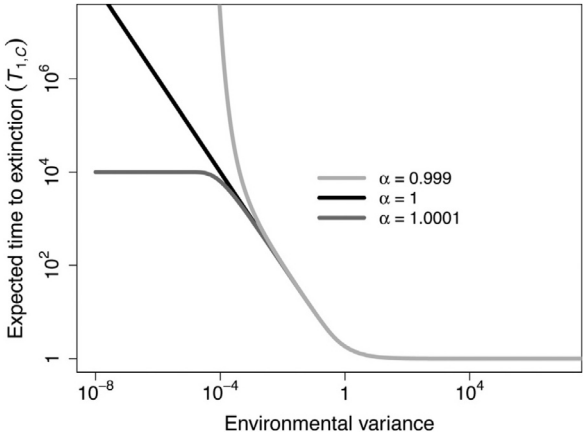


**Fig. 5.** Changes in expected extinction time for a species with initial abundance equal to one ($T_{1,C}$, also called the expected species lifetime) with increasing strength of environmental variance ($1/\lambda'$), when the changes in species log-abundances are specified by a truncated ALD. The values of $T_{1,C}$ are computed using (19) with $\alpha = 0.999$ or $\alpha = 1.0001$. The values of $T_{1,C}$ corresponding to the case $\alpha = 1$ are shown for comparison.

Analogous to previous studies that have used the non-zero sum neutral model (Volkov et al., 2003; Volkov et al., 2007; Chisholm and ODwyer, 2014), we now consider a null community model with temporal environmental variance, based on our population model. Specifically, to interpret our results in a community context in the sense described above, we introduce a speciation process. The simplest way of doing this is by adding a constant number of species to the community in each time-step, representing a constant speciation rate $\nu$. This assumption reflects constant immigration of new species arising from mostly time-invariant exogenous sources, such as a large metacommunity, and follows stochastic models by Etienne et al. (2007) and Fung et al. (2016b). In this case, considering discrete log-abundance states, the expected number of species in the community in state $i$ is specified by

$$S_i = \nu \sum_{t=0}^{\infty} p_{0i}(t) = \nu h_i, \tag{21}$$

where $p_{0i}(t)$ is the probability of a species going from state 0 to $i$ in time $t$. Therefore, the expected species richness of the community is

$$S = \nu \sum_{i=0}^{k} h_i = \nu T_1, \tag{22}$$

which in the continuous abundance limit gives $S_C = \nu T_{1,C}$. We see that $S_C$ is simply a constant multiple of $T_{1,C}$ and hence decreases with the strength of environmental variance ($1/\lambda'$) in the same way as $T_{1,C}$ (Figs. 4 and 5).

## 4. Discussion

Species populations are exposed to a wide variety of environmental disturbances, which can cause temporal fluctuations in species abundances and thereby influence changes in community-level diversity. Our contribution here has been to provide a new population model that can be explicitly solved for the relationship between environmental variance and extinction time. We find that extinction time generally declines with environmental variance in our model, representing greater stochastic extinction risk. This result, in conjunction with those of related models, contributes to a general picture of the circumstances in which we might expect to see negative versus positive effects of environmental variance on extinction time in nature.

There is a growing theoretical literature on the effects of temporal environmental variance on extinction risk, and the corresponding population models used vary in a few key ways. (i) Models differ in the degree of temporal correlation present in environmental variance. Most models focus on the low correlation limit of white noise or weakly colored noise, for reasons of analytical tractability. But natural disturbances such as droughts and storms can exhibit stronger temporal correlations, as evidenced directly from climate and oceanic data (Steele, 1985; Halley, 1996; Inchausti and Halley, 2002), and indirectly from population time-series (Pimm and Redfearn, 1988; Ariño and Pimm, 1995; Inchausti and Halley, 2002). There is thus a need for models that allow weak to strong temporally correlated environmental variance (colored noise). (ii) Models vary in their assumptions about the distribution of environmental effects on changes in population abundances, which can take different functional forms. (iii) Models vary

in their treatment of demographic variance: it is ideally treated explicitly but can be treated implicitly or ignored as a first approximation.

Our main contribution here is a new Markov chain model that includes environmental variance with an arbitrary degree of temporal correlation and yields an analytical formula for the relationship between environmental variance and extinction time (hence addressing point (i) above). The main limitation of our model in comparison with other population models is our implicit treatment of demographic variance (point (iii) above). We now discuss the main results of our model in the context of other published models, and then outline how its limitations could be overcome.

Our model typically exhibits negative relationships between environmental variance and expected extinction time. These negative relationships are consistent with previously published population models (Leigh, 1981; Lande, 1993; Foley, 1994; Kamenev et al., 2008). Our model also reproduces more specific results from some of these other models (Lande, 1993; Foley, 1994): in the case of a near-symmetric distribution of environmental effects on changes in species log-abundances, when starting with a species at its carrying capacity, we find a quadratic scaling of expected extinction time with the logarithm of species carrying capacity and an inverse scaling of expected extinction time with a measure of the strength of environmental variance. These scalings were also found in a two-species model where the environment changes periodically, with linear effects of the environment on species recruitment or mortality rates (first model of Hidalgo et al., 2017). In contrast, for sufficiently strong environmental variance, the model of Kamenev et al., 2008 predicts that expected extinction time scales independently of the species carrying capacity, which appears to be counter-intuitive. In all these models, more environmental variability means larger fluctuations in population abundances, which bring the abundances closer to the extinction threshold and hence increases the extinction risk, ultimately lowering extinction time.

Given the negative extinction time-environmental variance relationships in most population models, it is reasonable to consider negative relationships as the default and ask what mechanisms could induce positive relationships. One possibility is asymmetry in effects of environmental variance on changes in population abundances. If the asymmetry is such that population abundances become more likely to increase than decrease with increasing strength of environmental variance, then this could prolong the expected time to extinction. This asymmetry mechanism may be responsible for the positive extinction time-environmental variance relationship of Fung et al. (2016b). Although environmental effects on per-capita birth and death rates are symmetric in this model, the effects are filtered through demographic variance, leading to a distribution of population changes that is asymmetric and skewed towards increasingly larger positive values as the strength of environmental variance increases (Appendix F in Supplementary material). In contrast, we found evidence that this skewness was largely absent in our present model (Appendix F in Supplementary material), and we conjecture that this is because of the imposition of a species carrying capacity in our model and/or the lack of explicit demographic variance. In summary, asymmetric environmental effects can lead to positive extinction-environmental variance relationships (e.g., Fung et al., 2016b), but only under certain conditions.

In comparison with community models that explicitly model more than one species dynamically interacting with each other, our population model is limited because it is unable to explicitly represent interspecific interactions. If we consider an idealized community with no interspecific interactions and a constant speciation rate, then the negative extinction time-environmental variance relationship found from our population model directly implies a negative species richness-environmental variance relationship. Against this null case, there is a need to consider community mechanisms that could instead produce a positive relationship between temporal environmental variance and species richness. One possible mechanism is “storage effects”. These effects arise when (a) species in a community respond differently to environmental variance, (b) species exhibit buffered population growth and (c) there is a negative covariance between environmental and competition effects on species (Chesson, 1994, 2000). Together, these factors can generate a rare-species advantage and hence promote longer coexistence times (Chesson, 1994, 2000) and higher species richness. Recent modeling studies confirm that storage effects can allow environmental variance to have positive effects on species richness, but only when environmental variance is sufficiently weak (Adler and Drake, 2008; Danino et al., 2016). If the magnitude (Adler and Drake, 2008) and/or temporal correlation (Danino et al., 2016; second model of Hidalgo et al., 2017) of environmental variance are too strong, the effects of greater stochastic extinction risk predominate and the negative richness-environmental variance relationships re-emerge. A limitation of the analytical models used to explore storage effects (Danino et al., 2016; second model of Hidalgo et al., 2017) is that they are derived using diffusion approximations of master-equations, which may produce substantial errors for portions of the parameter space (Figs. 2 and 4 of Hidalgo et al., 2017).

As noted earlier, a major limitation of our model is that it does not contain storage effects or, indeed, any kind of interspecific interaction. Given the potential importance of these interactions for generating positive effects of environmental variance on extinction times, a future priority should be to incorporate them into our Markov chain framework. Another limitation of our model is the implicit representation of demographic variance through a binary extinction threshold, rather than as an explicit sampling process. Future progress in these directions will hopefully lead to a more sophisticated model that produces a richer variety of extinction time-environmental variance relationships, while retaining analytical tractability.

In summary, there is a substantial theoretical literature on the relationship between temporal environmental variance and extinction time, and it is clear that the relationship can be either negative or positive. A goal now is to gain an even deeper understanding of the mechanisms that give rise to negative versus positive relationships, so that we can ultimately predict when each type of relationship will prevail in nature. To this end, it is important to study a variety of mechanistic models, and to classify models according to which mechanisms they contain and what effects these mechanisms have on extinction time. Our main contribution here has been to introduce a new model of how extinction time changes with environmental variance, which is novel in its treatment of colored environmental noise in an analytically tractable way.

## Acknowledgements

We thank two anonymous reviewers for reading this manuscript and providing constructive comments, which have resulted in substantial improvements. RAC and TF are supported by the National University of Singapore grant WBS R-154-000-A10-720. JOD acknowledges the Simons Foundation Grant #376199 and the McDonnell Foundation Grant #220020439.

## Supplementary material

Supplementary material associated with this article can be found, in the online version, at https://doi.org/10.1016/j.ecocom.2017.09.006.

## References


Adler, P.B., Drake, J.M., 2008. Environmental variation, stochastic extinction, and competitive coexistence. Am. Nat. 172, E186–E195.

Ahlgren, I.F., Ahlgren, C.E., 1960. Ecological effects of forest fires. Bot. Rev. 26, 483–533.

Ariño, A., Pimm, S., 1995. The nature of population extremes. Evol. Ecol. 9, 429–443.

Bagchi, R., et al., 2014. Pathogens and insect herbivores drive rainforest plant diversity and composition. Nature 506, 85–88.

Brémaud, P., 1999. Markov Chains: Gibbs Fields, Monte Carlo Simulation, and Queues. Springer, New York pp. 445.

Ceballos, G., Ehrlich, P.R., Barnosky, A.D., García, A., Pringle, R.M., Palmer, T.M., 2015. Accelerated modern human-induced species losses: entering the sixth mass extinction. Sci. Adv. 1, e1400253.

Chesson, P., 1994. Multispecies competition in variable environments. Theor. Popul. Biol. 45, 227–276.

Chesson, P., 2000. Mechanisms of maintenance of species diversity. Annu. Rev. Ecol. Syst. 31, 343–366.

Chisholm, R.A., O'Dwyer, J.P., 2014. Species ages in neutral biodiversity models. Theor. Popul. Biol. 93, 85–94.

Chisholm, R.A., et al., 2014. Temporal variability of forest communities: empirical estimates of population change in 4000 tree species. Ecol. Lett. 17, 855–865.

Comita, L.S., Muller-Landau, H.C., Aguilar, S., Hubbell, S.P., 2010. Asymmetric density dependence shapes species abundances in a tropical tree community. Science 329, 330–332.

Connell, J.H., 1971. On the role of natural enemies in preventing competitive exclusion in some marine animals and in rain forest trees. In: den Boer, P.J., Gradwell, G.R. (Eds.), Dynamics of Populations. Centre for Agricultural Publishing and Documentation, Wageningen, The Netherlands, pp. 298–312.

Connell, J.H., 1997. Disturbance and recovery of coral assemblages. Coral Reefs 16 (Suppl), S101–S113.

Danino, M., Shnerb, N.M., Azaele, S., Kunin, W.E., Kessler, D.A., 2016. The effect of environmental stochasticity on species richness in neutral communities. J. Theor. Biol. 409, 155–164.

Etienne, R.S., Alonso, D., McKane, A.J., 2007. The zero-sum assumption in neutral biodiversity theory. J. Theor. Biol. 248, 522–536.

Foley, P., 1994. Predicting extinction times from environmental stochasticity and carrying capacity. Conserv. Biol. 8, 124–137.

Fung, T., O'Dwyer, J.P., Rahman, K.A., Fletcher, C.D., Chisholm, R.A., 2016. Reproducing static and dynamic biodiversity patterns in tropical forests: the critical role of environmental variance. Ecology 97, 1207–1217.

Fung, T., O'Dwyer, J.P., Chisholm, R.A., 2016. Species-abundance distributions under colored environmental noise. J. Math. Biol. 74, 289–311.

Gardner, T.A., Cote, I.M., Gill, J.A., Grant, A., Watkinson, A.R., 2005. Hurricanes and Caribbean coral reefs: impacts, recovery patterns, and role in long-term decline. Ecology 86, 174–184.

Halley, J.M., 1996. Ecology, evolution and 1/*f*-noise. Trends Ecol. Evol. 11, 33–37.

Harms, K.E., Wright, S.J., Calderón, O., Hernández, A., Herre, E.A., 2000. Pervasive density-dependent recruitment enhances seedling diversity in a tropical forest. Nature 404, 493–495.

Hidalgo, J., Suweis, S., Maritan, A., 2017. Species coexistence in a neutral dynamics with environmental noise. J. Theor. Biol. 413, 1–10.

Huntley, B., Midgley, G.F., Barnard, P., Valdes, P.J., 2014. Suborbital climatic variability and centres of biological diversity in the Cape region of southern Africa. J. Biogeogr. 41, 1338–1351.

Inchausti, P., Halley, J., 2002. The long-term temporal variability and spectral colour of animal populations. Evol. Ecol. Res. 4, 1033–1048.

Jackson, J.B.C., et al., 2001. Historical overfishing and the recent collapse of coastal ecosystems. Science 293, 629–638.

Janzen, D.H., 1970. Herbivores and the number of tree species in tropical forests. Am. Nat. 104, 501–528.

Kalyuzhny, M., Kadmon, R., Shnerb, N.M., 2015. A neutral theory with environmental stochasticity explains static and dynamic properties of ecological communities. Ecol. Lett. 18, 572–580.

Kamenev, A., Meerson, B., Shklovskii, B., 2008. How colored environmental noise affects population extinction. Phys. Rev. Lett. 101, 268103.

Knapp, A.K., et al., 2008. Consequences of more extreme precipitation regimes for terrestrial ecosystems. Bioscience 58, 811–821.

Lande, R., 1993. Risks of population extinction from demographic and environmental stochasticity and random catastrophes. Am. Nat. 142, 911–927.

Leigh, E.G., 1981. The average lifetime of a population in a varying environment. J. Theor. Biol. 90, 213–239.

Nee, S., 2005. The neutral theory of biodiversity: do the numbers add up? Funct. Ecol. 19, 173–176.

Ovaskainen, O., Meerson, B., 2010. Stochastic models of population extinction. Trends Ecol. Evol. 25, 643–652.

Pimm, S.L., Redfearn, A., 1988. The variability of population densities. Nature 334, 613–614.

Shurin, J.B., et al., 2010. Environmental stability and lake zooplankton diversity—contrasting effects of chemical and thermal variability. Ecol. Lett. 13, 453–463.

Steele, J.H., 1985. A comparison of terrestrial and marine ecological systems. Nature 313, 355–358.

Turcq, B., Sifeddine, A., Martin, L., Absy, M.L., Soubies, F., Suguio, K., Volkmer-Ribeiro, C., 1998. Amazonian forest fires: a lacustrine record of 7000 years. Ambio 27, 139–142.

Volkov, I., Banavar, J.R., Hubbell, S.P., Maritan, A., 2003. Neutral theory and relative species abundance in ecology. Nature 424, 1035–1037.

Volkov, I., Banavar, J.R., Hubbell, S.P., Maritan, A., 2007. Patterns of relative species abundance in rainforests and coral reefs. Nature 450, 45–49.

Wallace, A.R., 1878. Tropical Nature and Other Essays. Macmillan, New York and London pp. 356.

Webb, C.O., Gilbert, G.S., Donoghue, M.J., 2006. Phylodiversity-dependent seedling mortality, size structure, and disease in a Bornean rain forest. Ecology 87, S123–S131.